

Mechanism of Ca²⁺/Fe³⁺-based synergistic activation of quartz

Rongxiang Liu¹, Zhanfeng Yang^{1,3}, Jie Li², Qiang Li², Zhenjiang Wang¹, Xiaofeng Luo¹

¹ At the mining and coal School of Inner Mongolia University of Science and Technology, Baotou, 014010, China

² In the rare-earth School of Inner Mongolia University of Science and Technology, Baotou, 014010, China

³ Baotou Rare Earth Research Institute, Baotou, 014010, China

Corresponding author: 2842014603@qq.com (J. Li), yang_zhanfeng@163.com (Z. Yang)

Abstract: Although the flotation behaviors of iron concentrate and quartz are significantly different, quartz is the primary factor that affects the quality of iron concentrate. The flotation mechanism of quartz in the presence of mixed cationic Ca²⁺/Fe³⁺-co-activated SDS catcher was studied by conducting flotation tests with pure quartz mineral. The solution chemical calculation method, zeta potential calculation method, Fourier transform infrared (FT-IR) spectroscopy technique, X-ray photoelectron spectroscopy (XPS) technique, and other techniques were used to conduct the studies. The results showed that the maximum Ca²⁺/Fe³⁺-based synergistic activation of the flotation recovery process could be achieved in a certain range of pH values when three different activators were added sequentially. Analysis of the zeta potential values revealed that the Ca²⁺/Fe³⁺-activated quartz surface improved the extent of positive electricity generated and enhanced the SDS adsorption ability of the quartz surface. Results obtained using the FT-IR technique revealed that Ca²⁺/Fe³⁺ exerted a synergistic effect, and the adsorption process exploited the single oxygen bond interactions in the monovalent hydroxyl complex Ca(OH)⁺ and the double oxygen bond interactions in the Fe(OH)₃ precipitates. Results obtained using the XPS technique revealed that the synergistic effect exerted by Ca²⁺/Fe³⁺ was significantly stronger than that exerted by Ca²⁺ or Fe³⁺ alone. The stable Fe-based six-membered chelate ring was formed on the surface of quartz when Fe³⁺ was the activator, and the chain-like Ca-based complex was formed when Ca²⁺ was the activator. The adsorption process on the surface of quartz proceeded following chemical as well as physical adsorption pathways. The results revealed that Ca(OH)⁺ and Fe(OH)₃ played prominent roles during the activation of quartz surfaces in the presence of Ca²⁺/Fe³⁺.

Keywords: quartz, flotation, co-activation, metal ions, sodium dodecyl sulfonate

1. Introduction

The Bayan Obo mine is rich in rare earth metals and niobium. The value of the super-fine iron powder produced in this mine is significantly higher than that of ordinary super-iron powder [1]. A combination of grinding, magnetic separation and flotation methods is usually used to reduce the silica content in ultra-pure iron concentrates [2]. Numerous researchers have studied the flotation desilication process, primarily focusing on the flotation reagents used, the flotation process, and the flotation mechanism [3-6]. The process of flotation of quartz can be studied following two methods. In one of the methods, amine collectors are used to study the flotation of quartz, and the other method involves the use of multivalent metal ions to activate the surface of the quartz sample. The quartz activation step is followed by the use of anionic collectors for flotation [7]. To date, a consensus has not been reached on the mechanism of activation associated with polyvalent metal ions. Wang et al. [8] have reported that the process of hydroxide precipitation can be used to activate quartz in the presence of anionic collectors. Shi et al. [7] reported that the anion collector reacted with Ca(OH)₂ precipitates on the surface of the quartz sample, and this helped in realizing quartz floatation. Clark et al. [9] reported that Ca(OH)⁺ adsorbed on the surface of the quartz sample activated the system, resulting in flotation. Ca(OH)₂ was formed during

the process, the compound desorbed from the surface of the quartz sample, and flotation could not be realized under these conditions. Fuerstenua MC and Ejtemaei [10-11] reported that monovalent hydroxyl ions activated quartz in the flotation system. Al^{3+} , Fe^{3+} , and other expensive metal ions with small radii could be used to activate quartz. The activation mechanism followed in the presence of these ions has been globally and widely studied [12-14]. The effect of using a combination of metal ions on quartz flotation was studied using theoretical techniques. The results obtained by us were different from the results obtained using traditional methods which involved the use of single metal ions.

We selected sodium dodecyl sulfonate (SDS) as the anionic quartz collector, and the effects of Ca^{2+} , Fe^{3+} , and $\text{Ca}^{2+}/\text{Fe}^{3+}$ on quartz were investigated. Subsequently, the activation mechanism was studied in the presence of Ca^{2+} , Fe^{3+} , and $\text{Ca}^{2+}/\text{Fe}^{3+}$ by conducting the micro flotation and solution chemical tests. The zeta potential was analyzed, and the FT-IR and XPS techniques were used to arrive at the results.

2. Materials and methods

2.1. Materials

Pure quartz (SiO_2) was produced by the Bazhou Chemical Branch of the Tianjin Quartz Bell Factory. Powder X-ray diffraction (XRD) spectra of quartz were recorded (Fig. 1). The purity was 99.8%, and the possibility that metal cations might be present in the system was neglected. The samples were subjected to sieving (-0.074 mm) and drying processes. Analytically pure chemical agents such as FeCl_3 (purity: 99%, manufacturer: Tianjin Kuanzhong Fine Chemical Plant) and CaCl_2 (purity: 99.9%, manufacturer: Jining Huakai Resin Co., LTD.) were used to conduct the studies. SDS was used as the quartz collector. The pH of the experimental solutions was regulated using 5% HCl (HCl by volume or NaOH by weight), and deionized water (produced in the laboratory) was used for the experiments.

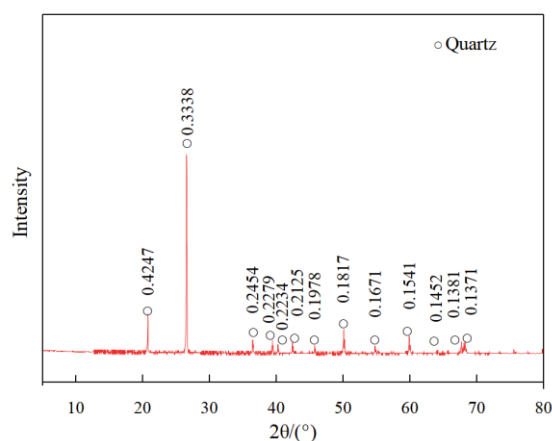


Fig 1. Powder X-ray diffraction (XRD) patterns recorded for quartz

The XFGC-II-type aerated system, hanging trough flotation machine (Jilin mineral exploration machinery factory), a drying box, a vacuum filter, and a balance were used to conduct the tests.

2.1. Methods

Pure mineral (2 g) was placed inside the flotation tank, and pH regulators (HCl or NaOH), activating agents (solutions of CaCl_2 or FeCl_3), and the collector (SDS) were mixed with the mineral. Deionized water was gradually added to the mixture under conditions of constant stirring. The cations were introduced into the system by adding (1) deionized water, (2) Ca^{2+} (concentration $3 \times 10^{-4} \text{ mol}\cdot\text{L}^{-1}$), (3) Fe^{3+} (concentration $3 \times 10^{-4} \text{ mol}\cdot\text{L}^{-1}$), and a combination of (4) Ca^{2+} (concentration $3 \times 10^{-4} \text{ mol}\cdot\text{L}^{-1}$) and Fe^{3+} (concentration $3 \times 10^{-4} \text{ mol}\cdot\text{L}^{-1}$). The concentration of SDS was $5 \times 10^{-4} \text{ mol}\cdot\text{L}^{-1}$ (based on literature reports [12-14]). The product was collected following the process of micro-flotation, and the collection process was allowed to proceed for 3 min. The foaming product and the product in the tank were weighed, and the extent of flotation recovery realized was determined as follows:

$$R = \frac{m_1}{m_1 + m_2} \times 100\% \quad (1)$$

where R denotes the flotation recovery, m_1 is the foamed product concentrate, and m_2 is the product tailings in the tank.

Detection methods: The pH of the system was measured using the PHS-3 pH meter (Shanghai Science Instrument Company), and the change in the surface potential was measured using the Zeta Plus Zeta potential analyzer (Brookhaven Company). The Vt-70 Fourier transform leaf infrared spectrometer (Burker company) was used to record the infrared spectra before and after the minerals reacted with the reagents. The XPS profiles for the quartz samples were recorded using the ESCALAB2250Xi Photoelectric Energy Spectrometer manufactured by Thermo Fisher Scientific, USA. A $K\alpha$ (1486.6 eV) line was used for anode excitation. The energy corresponding to the wide sweep profile was 100 eV, and the step length was maintained at 1 eV. The energy corresponding to the narrow sweep profile was 20 eV, and the step length was 0.05 eV. The 1s electron (284.6 eV) of C was selected as the internal standard to calibrate the energy spectrum. Avantage v5.52 was used to analyze XPS data. This system can also be used for data acquisition, quantitative analysis, element identification, peak-splitting fitting, etc. The corrected energy spectrum was used for peak-splitting and fitting. References for peak binding energies [16-23] (the binding energies corresponding to C1s [17-21], S2p [18-23], and O1s electrons [19-22]) were obtained from literature reports.

3. Results and discussion

3.1. Flotation tests for pure minerals

3.1.1. Effect of metal ions on quartz flotation studied under conditions of varying pH conditions

Analysis of Fig. 2 reveals that SDS does not influence the flotation behavior of quartz in the absence of cations. In the presence of Ca^{2+} , SDS significantly affects the flotation behavior of quartz, and approximately 68.4% of the material can be recovered at a pH of 12. Low amounts of quartz could be recovered at all other pH conditions, indicating that pH affected the surface electrical properties of quartz. SDS significantly affected the flotation behavior of quartz in the presence of Fe^{3+} when pH was in the range of 6-7. Approximately 88.3% of quartz was recovered under these conditions, and it was observed that the extent of flotation recovery decreased when a strong acid or base was used during the process. The decrease in the flotation recovery could be attributed to the fact that the pH of the solution influenced the surface electrical properties of quartz. The flotation of quartz was significantly affected by the presence of SDS when the $\text{Ca}^{2+}/\text{Fe}^{3+}$ system was used as the additive at a pH of 8. Approximately 97.3% of quartz could be recovered under these conditions. It was observed that >90% of quartz could be recovered in the pH range of 6-9. The results revealed that the synergistic effect exerted by pH and the cations in the presence of SDS helped improve the flotation behavior of quartz. The effect was exerted following the hydrolysis of $\text{Ca}^{2+}/\text{Fe}^{3+}$, and these ions could jointly activate the quartz surface. The pH range widened when the mixed-ion system was used for surface activation. The extent of quartz activation realized in the presence of the $\text{Ca}^{2+}/\text{Fe}^{3+}$ dual system was better than that realized when either Ca^{2+} or Fe^{3+} was used for sample activation. The samples could be efficiently activated over a wide pH range, and this made controlling the pH of the solution easy.

3.1.2. Influence of the concentration of different activators on the flotation behavior of quartz

The concentration of the anionic collector was maintained at $5 \times 10^{-4} \text{ mol} \cdot \text{L}^{-1}$. The cationic modifier was selected by (1) adding only Ca^{2+} (pH 12), (2) adding only Fe^{3+} (pH 7), and (3) adding a mixture containing Ca^{2+} and Fe^{3+} ($\text{Ca}^{2+} : \text{Fe}^{3+} = 1:1$) at pH 8. The flotation recovery recorded during the floatation of quartz under conditions of varying concentrations of the activators are presented in Fig. 3.

Analysis of Fig. 3 reveals that the concentration of the metal ions significantly affects the flotation behavior of quartz. The quartz recovery rate was 75.8% when the concentration of Ca^{2+} was $5 \times 10^{-4} \text{ mol} \cdot \text{L}^{-1}$. The flotation recovery remained unchanged when the concentration of the cation was increased. Approximately 89.3% of quartz could be recovered when the concentration of the Fe^{3+} activator was $5 \times 10^{-4} \text{ mol} \cdot \text{L}^{-1}$. The extent of flotation recovery did not increase with an increase in the cation concentration. The flotation recovery increased when the concentration of the mixture consisting of Ca^{2+}

and Fe^{3+} ($\text{Ca}^{2+}:\text{Fe}^{3+}=1:1$) was increased (as shown by the broken line). The maximum recovery rate (97.2%) for quartz was recorded when the concentration of the mixed system was $5 \times 10^{-4} \text{ mol}\cdot\text{L}^{-1}$. The results revealed that the synergistic effect exerted by Ca^{2+} and Fe^{3+} resulted in good recovery rates. The extent of quartz recovered using the mixed system was higher than the extent of flotation recovery achieved using individual metal ions. It was observed that the flotation recovery was close to 100% was the mixed system was used.

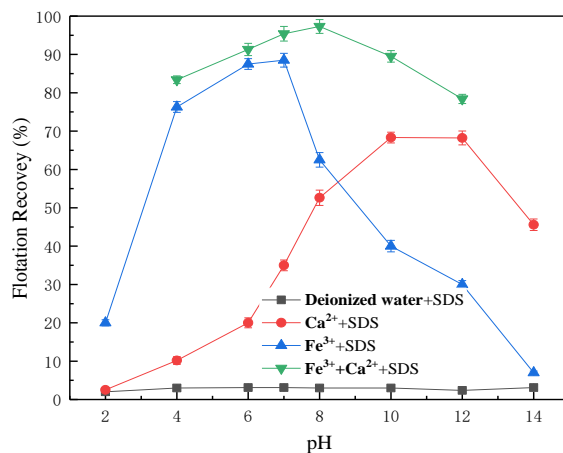


Fig. 2. Effect of metal ions on quartz flotation at different pH values

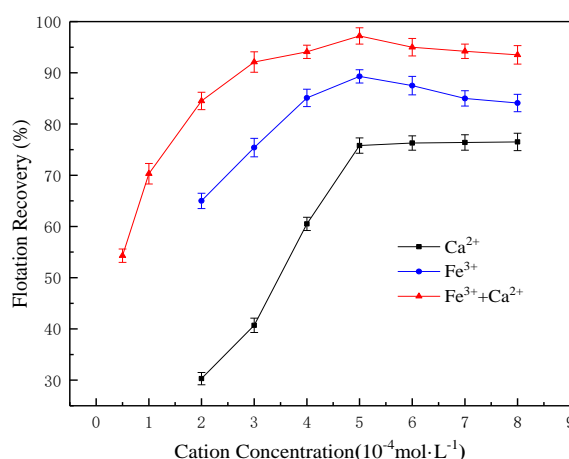


Fig. 3. Effect of the activator concentration on the extent of quartz flotation

3.1.3 Effect of SDS concentration on the flotation behavior of quartz studied in the presence of different activators

The experimental conditions have been presented ((1) Ca^{2+} ($5 \times 10^{-4} \text{ mol}\cdot\text{L}^{-1}$, pH 12), (2) Fe^{3+} ($5 \times 10^{-4} \text{ mol}\cdot\text{L}^{-1}$, pH 12), (3) $\text{Ca}^{2+}:\text{Fe}^{3+} = 1:1$ (concentration: $5 \times 10^{-4} \text{ mol}\cdot\text{L}^{-1}$, pH 8)), and the flotation recovery recorded under different SDS concentrations are presented in Fig. 4.

Analysis of Fig. 4 reveals that the flotation recovery increases with an increase in the SDS concentration when different activating agents are added to the system. A stable flotation recovery was achieved, and 75.5% of quartz could be recovered when the concentration of SDS was $5 \times 10^{-4} \text{ mol}\cdot\text{L}^{-1}$ and Ca^{2+} was used as the additive. Approximately 90.5% of quartz could be recovered when the concentration of SDS was $5 \times 10^{-4} \text{ mol}\cdot\text{L}^{-1}$ and Fe^{3+} was used as the additive. Approximately 98.5% of quartz could be recovered when the mixed system ($\text{Ca}^{2+}:\text{Fe}^{3+} = 1:1$) was introduced into the system, and the concentration of SDS was $5 \times 10^{-4} \text{ mol}\cdot\text{L}^{-1}$. In conclusion, the optimum SDS concentration was $5 \times 10^{-4} \text{ mol}\cdot\text{L}^{-1}$, which agreed well with the experimental data. The concentration of SDS exerted little effect on the activity of the metal ions, which could get adsorbed on the surface of quartz and change the surface properties of the system. Thus, the metal ions promoted the flotation of quartz.

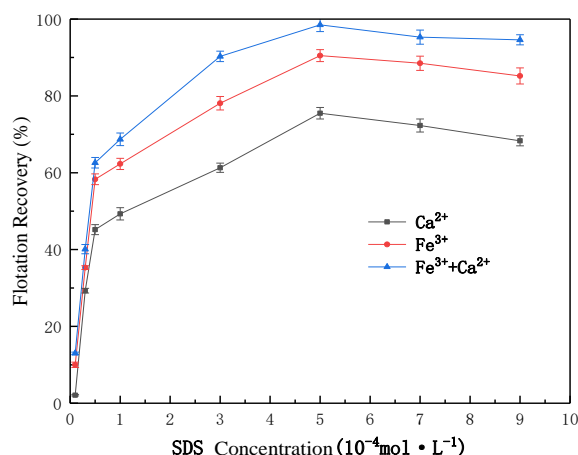


Fig. 4. Effect of sodium dodecyl sulfate (SDS) concentration on quartz flotation

3.2. Mechanism analysis

The mechanism of Ca^{2+} , Fe^{3+} , and $\text{Ca}^{2+}/\text{Fe}^{3+}$ -based activation processes observed during the flotation of quartz was analyzed by conducting solution chemical and zeta potential tests. The samples were also analyzed using the FT-IR and XPS techniques. We aimed to establish a theoretical basis for the surface activation of metal ions and quartz. It was observed that the effect of the $\text{Ca}^{2+}/\text{Fe}^{3+}$ system was higher than the effect exerted by a single cationic living fossil. We deduced the reason behind this phenomenon and explored the process of adsorption.

3.2.1. Solution chemical calculation

The solution equilibrium equation defining the process of cationic hydrolysis in pulp^[12] presents the relation between the concentration of each component in the solution and the pH of the solution ($\lg C\text{-pH}$). The relevant results are presented in Fig. 5 and Fig. 6 for Ca^{2+} and Fe^{3+} , respectively.

As seen in Fig. 5, calcium exists in an aqueous (_{aq}) solution in the form of Ca^{2+} ions, as hydroxyl complexes, and as hydroxyl compounds at high pH conditions (Fig. 5). Ca^{2+} , $\text{Ca}(\text{OH})^+$, and water-soluble $\text{Ca}(\text{OH})_2$ were the primary components in the system when the pH was <12.5 . It was observed that the concentration of $\text{Ca}(\text{OH})^+$ and water-soluble $\text{Ca}(\text{OH})_2$ (_{aq}) decreased with an increase in pH, and the concentration of $\text{Ca}(\text{OH})^+$ and water-soluble $\text{Ca}(\text{OH})_2$ (_{aq}) increased when the pH value was 12. $\text{Ca}(\text{OH})^+$ functioned as the activator under these conditions, as it was the dominant component in the solution. When the pH was >12.5 , the concentrations of $\text{Ca}(\text{OH})^+$ and $\text{Ca}(\text{OH})_2$ (_s) in the solution decreased, while the amount of $\text{Ca}(\text{OH})_2$ (_s) precipitated during the process increased. The extent of recovery of quartz realized decreased, and the results agreed well with the results obtained by conducting flotation tests.

Fig. 6 reveals that iron is present in its ionic state (Fe^{3+}) or as hydroxyl complexes ($\text{Fe}(\text{OH})_2^+$ and $\text{Fe}(\text{OH})_2^{2+}$) in the system when the pH is <2.4 . Precipitates were not formed under these conditions, but precipitates of $\text{Fe}(\text{OH})_3$ (_s) were formed when the pH was >2.4 . The Fe^{3+} content and the amount of the hydroxyl complexes ($\text{Fe}(\text{OH})_2^+$ and $\text{Fe}(\text{OH})_2^{2+}$) decreased rapidly with an increase in pH in the range of 7–9. The $\text{Fe}(\text{OH})_3$ (_s) precipitates were the dominant components, and these precipitates helped to activate quartz.

3.2.2. Analysis of the zeta potential

The degree of dissociation of the flotation reagents in water and the pH of the pulp can affect the zeta potential of minerals. This indicates that the activation mechanism can be understood by analyzing the zeta potential of the pulp. Quartz (0.5 g) was ground until the particle size was $<5 \mu\text{m}$. The ground samples were taken in small beakers, and deionized water was used to prepare sample slurries (50 mL). SDS and the activator (Ca^{2+} , Fe^{3+} , or $\text{Ca}^{2+}/\text{Fe}^{3+}$; concentration: $5 \times 10^{-4} \text{ mol} \cdot \text{L}^{-1}$) were added to the slurry, and the pH of the slurry was adjusted using an aqueous solution of HCl or NaOH. The prepared slurry

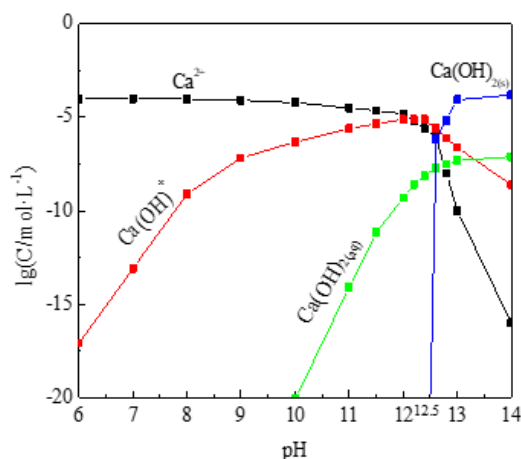


Fig. 5. lg C–pH diagram for Ca^{2+} hydrolysis ($\text{Ca}^{2+}=5\times 10^{-4} \text{ mol}\cdot\text{L}^{-1}$)

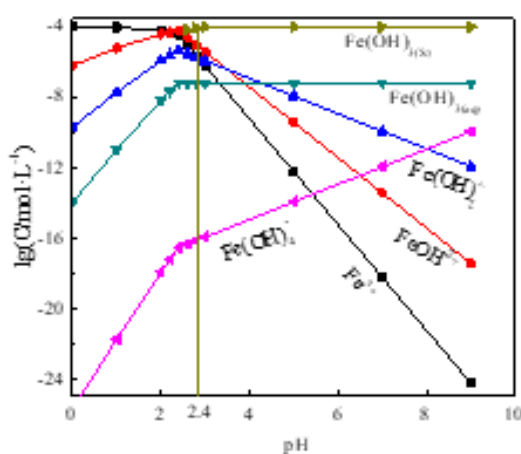


Fig. 6. lg C–pH diagram for Fe^{3+} hydrolysis ($\text{Fe}^{3+}=5\times 10^{-4} \text{ mol}\cdot\text{L}^{-1}$)

was stirred for 30 min (XFGC-II-type; aerated; hanging from the flotation machine; 3000 rpm), following which it was allowed to stand for 10 min. A zeta potential analyzer was used to measure the changes in the surface potentials of the samples (before and after the addition of SDS, Ca^{2+} , Fe^{3+} , and $\text{Ca}^{2+}/\text{Fe}^{3+}$). The surface potentials recorded at different pH values are presented in Fig. 7.

The point of zero charge (pzc) of quartz was recorded to be pH 2.5 in the absence of a flotation reagent (Fig. 7). The surface of quartz was negatively charged when the pH was in the range of 2.5–14. An increase in pH resulted in an increase in the concentration of OH^- . A decrease in the zeta potential indicates that the pH of the solution affects the concentration of the charged group on the surface of the mineral, resulting in changes in the surface potential of the sample. The interaction between the anionic collector and quartz resulted in a negative shift in the zeta potential of the system. The isoelectric point decreased under these conditions, indicating that the negatively charged sulfonate ions in SDS were adsorbed on the surface of the mineral. This eventually resulted in an increase in surface electronegativity. When Ca^{2+} , Fe^{3+} , and $\text{Ca}^{2+}/\text{Fe}^{3+}$ were introduced into the slurry, the cations were adsorbed on the surface of the quartz sample, resulting in an increase in the number of positive charges on the surface of the quartz sample.

The zeta potential of quartz shifted toward the square, and the isoelectric point increased when Ca^{2+} was introduced into the system at a pH >9.5. $\text{Ca}(\text{OH})^+$ was primarily adsorbed on the surface of quartz when the sample was present in a solution of Ca^{2+} (a positively charged solution). It was observed that the zeta potential of quartz increased under these conditions. Ca^{2+} and OH^- react to form $\text{Ca}(\text{OH})_2$ at a pH of >12. The $\text{Ca}(\text{OH})^+$ concentration decreased under these conditions, and a negative shift in the zeta potential was observed. The results revealed that the optimal pH range was 9.5–12. The surface potential of quartz increased in the presence of Fe^{3+} , and the isoelectric point increased when the pH

value was >4.1 . The results revealed that Fe^{3+} primarily existed in the solution as precipitates of $\text{Fe}(\text{OH})_3$ when the pH of the system was >2.4 . The pzc of $\text{Fe}(\text{OH})_3$ was recorded at a pH of 6.7^[24]. The material exhibited a strong adsorption capacity^[24], and it could be readily adsorbed on the surface of the quartz sample. The presence of $\text{Fe}(\text{OH})_3$ resulted in an increase in the number of active radicals on the quartz surface. The adsorption of the material on the surface of quartz resulted in an increase in the zeta potential of quartz. The OH^- concentration increased with an increase in the pH of the solution. When the pH was >8 , $\text{Fe}(\text{OH})_3$ reacted with OH^- to form $\text{Fe}(\text{OH})_4^-$. A large amount of $\text{Fe}(\text{OH})_4^-$ was adsorbed on the negatively charged quartz surface, and the zeta potential rapidly shifted to the negative direction under these conditions. The anionic SDS molecules were repelled under these conditions, resulting in a decrease in the floatability of quartz. The poor floatability of quartz can be associated with the degree of SDS dissociation at pH values less than 6^[24]. Therefore, the suitable pH range was found to be 4–11.

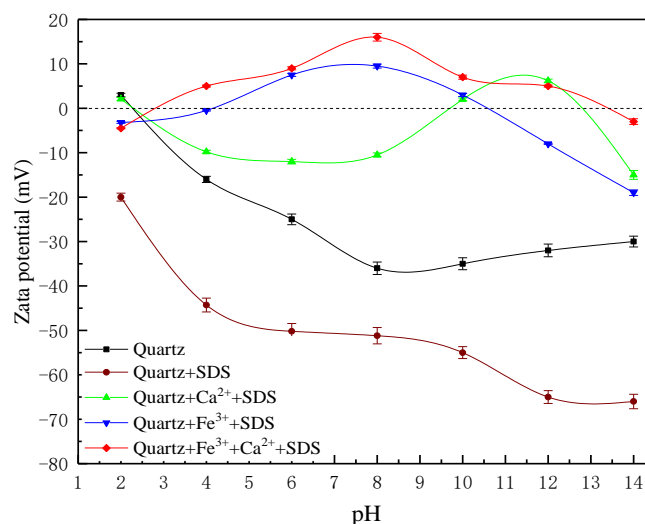


Fig. 7. Changes in the zeta potential with changes in the pH recorded before and after quartz interacted with the chemicals

A negative surface potential was recorded for the quartz surface when $\text{Ca}^{2+}/\text{Fe}^{3+}$ was added to the system at a $\text{pH} < 2.4$. When the pH value is 7, $\text{Fe}(\text{OH})_3$ functions as the primary Fe^{3+} -based activator of quartz. The Ca^{2+} -based activator does not affect the process, and Fe^{3+} hydrolysis occurs preferentially in the inner layer of quartz. This results in changes in the zeta potential and an increase in the adsorption forces. When $8 > \text{pH} > 7$, the number of OH^- ions in the solution increases, and these react with the $\text{Fe}(\text{OH})_3$ precipitates to form $\text{Fe}(\text{OH})_4^-$, resulting in a negative shift in the surface potential. The hydrolysis of the Ca^{2+} activator resulted in the formation of $\text{Ca}(\text{OH})^+$ as the dominant component, and this component promoted the activation of quartz. The rate of formation of $\text{Ca}(\text{OH})^+$ was higher than the rate of formation of $\text{Fe}(\text{OH})_3$. An overall upward shift in the potential of quartz was observed under these conditions. The results (Fig. 3) revealed that the rate of recovery increased, and the maximum value was recorded when the pH of the system was 8 (Fig. 7). $\text{Ca}(\text{OH})^+$ and $\text{Fe}(\text{OH})_3$ were simultaneously adsorbed on the surface of quartz under these conditions, and this process promoted the flotation of quartz in the presence of SDS. When $12.5 > \text{pH} > 8$, the concentration of OH^- in the solution increased, and a negative shift in the positive potential was observed. This could be attributed to the continuous generation of $\text{Fe}(\text{OH})_4^-$, which neutralized the electrical properties of the $\text{Ca}(\text{OH})^+$ units adsorbed on the quartz surface. Hence, the overall surface potential decreased, but the value remained >0 . It was observed that quartz could be recovered under these conditions. When $14 > \text{pH} > 12.5$, the surface of quartz remains negatively charged, and the products obtained following the hydrolysis of $\text{Ca}^{2+}/\text{Fe}^{3+}$ do not function as activators. The flotation recovery of quartz decreased under these conditions. It can be inferred that if the $\text{Ca}^{2+}/\text{Fe}^{3+}$ system is synergistically activated, the zeta potential corresponding to the surface of the quartz sample can be increased at pH 8. Thus, the activation process observed in the presence of the dual ion system is more efficient than the processes observed in the presence of individual ions. The extent of adsorption of SDS realized on the surface of quartz can be

improved under these conditions, and the process promotes the flotation of quartz.

3.2.3. FT-IR analysis

The FT-IR technique was used to analyze the samples to explore the adsorption state of the mineral surface before and after the introduction of the cation-activated quartz system and SDS.

Fig. 8 presents the infrared spectral profiles recorded before and after quartz interacted with the reagents. The absorption peak at 3437 cm^{-1} (Fig. 8a) can be attributed to the stretching vibration of the OH^- units in SDS. The intense absorption peaks at 2928 and 2857 cm^{-1} can be attributed to the stretching vibrations of the $-\text{CH}_2-$ and $-\text{CH}_3$ units [25]. The absorption peak at 1446 cm^{-1} can be attributed to the bending vibration of the $-\text{CH}_2-$ unit, and the characteristic peak of the sulfonate groups appears in the wavenumber range of $1200\text{--}950\text{ cm}^{-1}$ [25]. The absorption peaks at 1190 and 1042 cm^{-1} can be attributed to the antisymmetric and symmetric stretching vibrations of the $-\text{SO}_3^-$ group [25]. The absorption peak at 881 cm^{-1} corresponds to the stretching vibration of the S-OH group [25], and the absorption peak at 701 cm^{-1} corresponds to the stretching vibration of the S-O group [25]. The IR profiles recorded for quartz (Fig. 8b) were analyzed, and it was observed that the peak corresponding to the stretching vibration of the $-\text{OH}$ group in Si-OH appeared at 3437 cm^{-1} [25]. The broad and strong absorption peak appearing at 1085 cm^{-1} was attributed to the asymmetric stretching vibration of the Si-O group [25]. The symmetric stretching vibration of the Si-O group was reflected by the peak at 788 cm^{-1} [25]. The peak at 462 cm^{-1} was attributed to the symmetric variable angle vibration of the Si-O group [25]. New peaks were not observed in the profiles (Fig. 8c) recorded after the interaction of quartz with SDS. This indicated that the molecules were not adsorbed on the surface.

The IR profiles recorded for the quartz samples activated by Ca^{2+} at a pH of 12 in the presence of SDS are shown in Fig. 8d, and the IR profiles of the quartz samples activated using Fe^{3+} at a pH of 6 in the presence of SDS are presented in Fig. 8e. The IR profiles recorded at a pH of 8 for the quartz sample activated using $\text{Ca}^{2+}/\text{Fe}^{3+}$ (in the presence of SDS) are presented in Fig. 7f. The absorption peaks corresponding to the stretching vibrations of the $-\text{CH}_2-$ and $-\text{CH}_3$ groups appear at 2928 and 2857 cm^{-1} ,

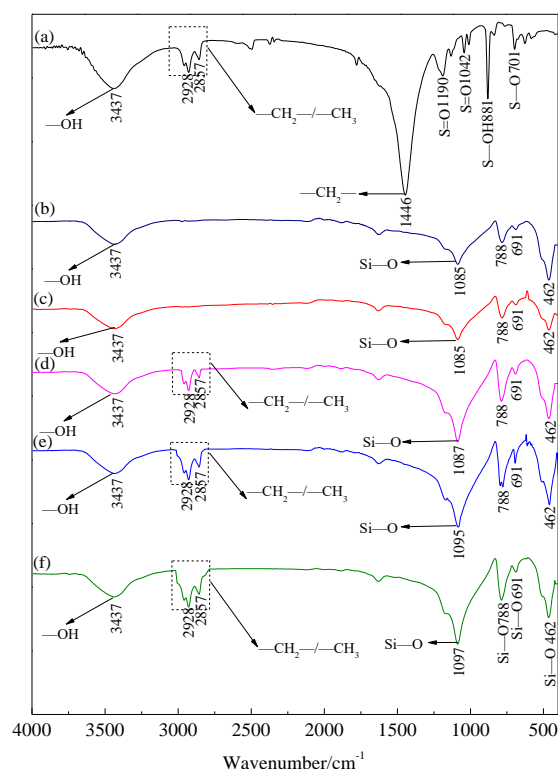


Fig. 8. FT-IR spectral profiles recorded for the samples before and after quartz interacted with the reagents (pH 8) ((a) SDS; (b) Quartz; (c) Quartz treated with SDS; (d) Ca^{2+} -activated quartz treated with SDS; (e) Fe^{3+} -activated quartz treated with SDS (f) $\text{Ca}^{2+}/\text{Fe}^{3+}$ -activated quartz treated with SDS)

respectively (Fig. 8d, e, and f), and the results agree well with the results presented in Fig. 8a. The peak positions remain unchanged, reflecting physical adsorption [26]. The intensity of the characteristic peak changed, and it was observed that the intensity of the absorption peak generated under conditions of Fe³⁺-based activation was higher than the intensity of the peak generated under conditions of Ca²⁺-based activation. This indicated that the number of functional groups associated with the physical adsorption of SDS realized in the presence of Fe³⁺ was higher than the number of functional groups exploited during the adsorption of SDS in the presence of Ca²⁺. Compared to the latter, a denser structure was formed in the case of the former. The peaks corresponding to the vibration of the Si-O group appeared at 1087, 1095, and 1085 cm⁻¹ (Figs. 8b, d, e, and f). The peak positions red-shifted by 2, 10, and 15 cm⁻¹, respectively, and the intensity of the peaks and the area under the peaks increased under these conditions. This indicated an increase in the number of groups adsorbed on the surface of the organic agent [25].

According to equation (2) [12], the energies corresponding to the Si-O asymmetric stretching vibration represented by the peak at 1085 cm⁻¹ in Fig. 7b, d, e, and f are 8.85×10¹³, 8.88×10¹³, 9.01×10¹³, and 9.05×10¹³ kJ mol⁻¹, respectively. The results reveal that the binding energy of quartz increases when Ca²⁺, Fe³⁺, and Ca²⁺/Fe³⁺ are used for activation (300 × 10⁹, 1600 × 10⁹, and 2000 kJ mol⁻¹, respectively). This indicates that the adsorption process proceeds via the chemical adsorption pathway exploiting a large number of functional groups when synergistic activation is realized in the presence of Ca²⁺/Fe³⁺.

$$\nu = \frac{1}{1307} \sqrt{\frac{K}{M}} \quad (2)$$

Here ν is the wave number, M is the relative molecular weight, and K is the bond energy. The surface state of quartz is closely related to the pH of the solution [12,15]. It was observed that the =Si-O- and =Si-OH groups were present at high and low pH conditions, respectively.

The results obtained by conducting various experiments revealed that the optimum pH for Ca²⁺-based quartz activation was 12. Under these conditions, the adsorption process proceeded by exploiting the mono-oxygen bonds in the monovalent hydroxyl complex. The bond between Ca(OH)⁺ and Si-O (on the quartz surface) breaks under these conditions, resulting in the formation of the Si-O-Ca (OH) unit as the active site [24]. The Ca²⁺ ions were adsorbed on the surface of the oxidized ore through the monovalent hydroxyl complex, and the metal ions bonded with the oxygen atoms present on the surface. The bonds forged under these conditions were not significantly strong. The change in the binding energy was small (300 × 10⁹ kJ · mol⁻¹), and this was inferred by analyzing the IR profiles. Efficient adsorption was realized on Fe³⁺-activated quartz at a pH of 7. The adsorption process proceeded under these conditions through the formation of chelates in the presence of Fe(OH)₃ precipitates. The breakage of the bonds between the Fe(OH)₃ precipitates and the Si-OH units on the surface of the quartz results in the formation of the Si-O-Fe (OH)⁺ units as the active sites. Thus, two oxygen atoms could be introduced on the surface of quartz following the completion of the reactions. The binding energy changed significantly post chelation (1600 × 10⁹ kJ · mol⁻¹), and analysis of the IR profiles revealed that the strength of the adsorption process was higher than that of the process reported in the previous section. The maximum recovery rate for quartz and the maximum positive surface potential were recorded when the pH of the system was 8. The results revealed that Ca(OH)⁺ and Fe(OH)₃ were the dominant components in the Ca²⁺/Fe³⁺-activated quartz sample. Si-O-Ca(OH) and Si-O-Fe(OH)⁺ functioned as active sites, and these units affected the adsorption process simultaneously. The absence of a new peak in Fig. 8f indicated that chemical reactions did not occur under these conditions. Chemical adsorption was achieved, and the characteristic peaks corresponding to Si-O red-shifted by 12 cm⁻¹. The increase in the intensity of the characteristic peak for Si-O indicated an increase in the extent of adsorption. The binding energy increased by 2000 × 10⁹ kJ mol⁻¹, indicating the progress of the chemical adsorption process. The characteristic peaks corresponding to the -CH₂- and -CH₃ groups appeared at 2928 and 2857 cm⁻¹, respectively. The peak positions and bond energy remained unaltered post adsorption, indicating that the extent of physical adsorption increased with an increase in the number of adsorbed groups.

In summary, it can be stated that the use of Ca²⁺, Fe³⁺, and Ca²⁺/Fe³⁺ as additives can help improve the extent of SDS adsorption realized on quartz. The synergistic effect exerted by Ca²⁺ and Fe³⁺ was stronger than the effect exerted by a single metal ion. Si-O-Ca (OH) and Si-O-Fe (OH)⁺ were generated

as the active sites under conditions of synergistic activation, and these sites simultaneously influenced the adsorption process. Physical as well as chemical adsorption processes were associated with the SDS adsorption process under conditions of synergistic activation.

3.2.4. Analysis of XPS profiles

The XPS technique is used to study the electron binding energy of the inner layer of a substance to determine the chemical state of the element. This technique is primarily used for the qualitative analysis of chemical elements, the qualitative or semi-quantitative analysis of surface elements, and the chemical valence state analysis of elements. XPS profiles were recorded for the samples under study. The profiles were recorded in the presence and absence of different activators to analyze the interactions between quartz and the reagents. The full XPS profile is presented in Fig. 9.

Peaks corresponding to Si2s, Si2p, O1s, OKL1, and C1s are presented in Fig. 9a. Analysis of the profiles indicated that the quartz sample was pure and devoid of metal impurities. The profiles corresponding to S2s, S2p, Na1s, NaKL1, O1s, OKL1, and C1s in SDS are presented in Fig. 9b. Fig. 8a and Fig. 9b were compared, and the formation of new peaks was not observed (Fig. 9c). However, a change in the binding energy and elemental composition was recorded. The results are presented in Table 1. Analysis of the data reveals that the binding energies corresponding to the Si2p, Si2s, O1s, and C1s units in the quartz ore differed from the binding energies of the corresponding units in the SDS-adsorbed sample by 0.03, 0.2, 0.01, and 0.04 eV, respectively. The displacement values were within the range of instrumental error (0.3 eV), indicating that SDS did not significantly affect the binding energies associated with the inner electrons in quartz. Finally, the results revealed that SDS was not adsorbed on quartz.

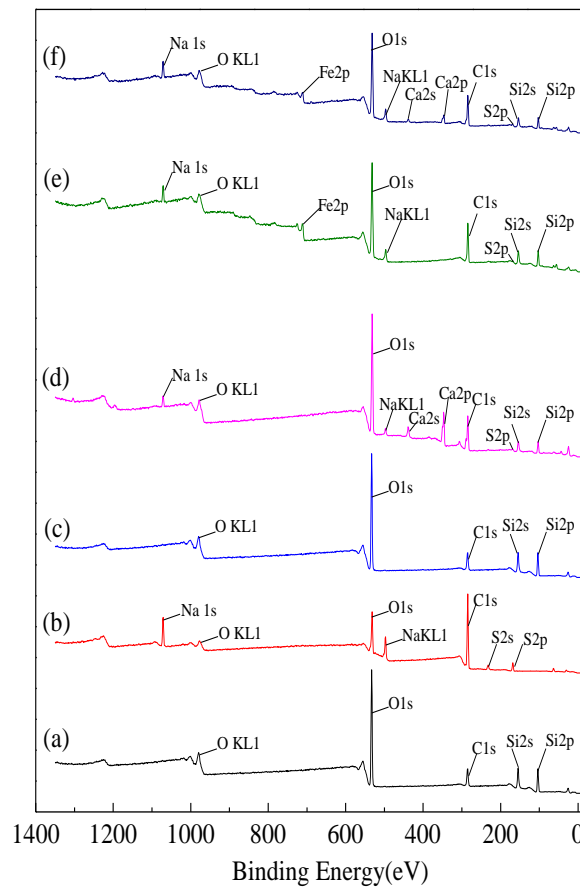


Fig. 9. XPS profiles recorded for quartz (before and after chemical treatment) (a) Quartz; (b) SDS; (c) Quartz treated with SDS; (d) Ca²⁺-activated quartz treated with SDS; (e) Fe³⁺-activated quartz treated with SDS; (f) Ca²⁺/Fe³⁺-activated quartz treated with SDS)

Table1. Atomic orbital binding energy and the atomic fraction of elements recorded before and after quartz reacted with different agents

Elements	O1s		C1s		Si2p		Si2s		Ca2p		Fe2p		S2p	
	Binding energy /eV	Atomic number scores /%	Binding energy /eV	Atomic number scores /%	Binding energy /eV	Atomic number scores /%	Binding energy /eV	Atomic number scores /%	Binding energy /eV	Atomic number scores /%	Binding energy /eV	Atomic number scores /%	Binding energy /eV	Atomic number scores /%
a	532.98	34.98	285.29	17	103.83	18.84	154.87	18.12	-	-	-	-	-	-
b	531.76	19.71	284.94	35	-	-	-	-	-	-	-	-	168.46	4.40
c	532.97	34.76	285.25	16.63	103.86	18.45	154.67	18.3	-	-	-	-	-	-
d	531.72	33.64	284.85	30.67	103.21	9.85	154.13	9.3	346.93	6.55	-	-	167.66	1.34
e	531.92	30.75	284.7	30.51	103.04	14.17	154.01	12.55	-	-	711.16	2.05	167.59	1.38
f	531.74	32.16	284.74	29.47	102.92	11.16	153.9	10.69	346.90	2.32	711.32	2.11	167.00	1.75

The interaction between quartz and Ca^{2+} and SDS is shown in Fig. 9d. New peaks corresponding to Ca2p, S2p, Na1s, and NaKL1 appeared in the profiles, indicating adsorption. Analysis of the data presented in Table 1 revealed that the binding energy corresponding to Ca2p was 346.93 eV, and the element fraction was 6.55%. The binding energy corresponding to S2p was 167.66 eV, and the element fraction was 1.34%. Compared with the S2p binding energy in XPS of SDS, the chemical shift of the S2p binding energy was 0.8 eV. Analysis of the XPS profile recorded for the Ca^{2+} -activated quartz sample revealed that the chemical shift for the binding energy of Si2s was 0.74 eV, and the element fraction was 9.3%, the chemical shift for the binding energy of Si2p was 0.62 eV, and the element fraction was 9.85%, the chemical shift for the binding energy of O1s was 1.26 eV, and the element fraction was 33.64% (which was 1.34% lower than the element fraction recorded for raw ore), and the chemical shift for the binding energy of C1s was 0.44 eV, and the element fraction was 30.67% (which was 13.67% higher than the element fraction recorded for raw ore). The fractions of Si2s and Si2p in quartz decreased significantly, indicating the chemical adsorption of Ca^{2+} on the surface of quartz and the formation of the Si-O-Ca(OH) bond. The Si-O-Ca(OH) bond participated in the adsorption process through the S2p orbitals in SDS, and the outer hydrophobic layer of SDS could readily float under these conditions.

The profiles recorded post the interaction of quartz with SDS under conditions of Fe^{3+} activation are presented in Fig. 8e. New spectral lines corresponding to Fe2p, S2p, Na1s, and NaKL1 appeared in the profiles, indicating the progress of the adsorption process. Analysis of the data presented in Table 1 revealed that the binding energy corresponding to Fe2p on the quartz surface was 711.16 eV, and the element fraction was 2.05%. The binding energy corresponding to S2p was 167.59 eV, and the element fraction was 1.38%. The chemical shift for the binding energy of S2p was recorded to be 1.35 eV. For the Fe^{3+} -activated quartz system, the chemical shift for the binding energy of Si2s was 0.86 eV, and the element fraction was 12.55%. The chemical shift for the binding energy of Si2p was 0.79 eV, and the element fraction was 14.17%. The chemical shift for the binding energy of O1s was 1.06 eV, and the element fraction was 30.75% (which was 4.23% lower than the element fraction recorded for the ore). The chemical shift for the binding energy of C1s was 0.59 eV, and the element fraction was 30.51% (which was 13.51% higher than the fraction recorded for the raw ore sample). The element fraction corresponding to Si2s and Si2p decreased significantly (compared to the element fractions in quartz), indicating that Fe^{3+} was chemically adsorbed on the surface of quartz [29]. The Si-O-Fe (OH)⁺ bond was formed, and the chemical adsorption of the Si-O-Fe (OH)⁺ unit proceeded through the S2p unit in SDS.

The activation of quartz by the $\text{Ca}^{2+}/\text{Fe}^{3+}$ system in the presence of SDS was studied (Fig. 8f). New peaks corresponding to Ca2p, Fe2p, S2p, Na1s, and NaKL1 appeared in the profiles, indicating that the cations were chemically adsorbed on quartz. Analysis of the data presented in Table 1 revealed that the binding energy corresponding to Fe2p (for quartz) was 711.32eV, and the element fraction was 2.11%. The binding energy corresponding to Ca2p was 346.90 eV, and the element fraction was 2.32%. The binding energy corresponding to Si2p was 168.00 eV, and the element fraction was 1.75%. The XPS

profile recorded for the $\text{Ca}^{2+}/\text{Fe}^{3+}$ -co-activated quartz system was analyzed, and it was observed that the chemical shift for the binding energy of Si2s was 0.97 eV, and the element fraction was 10.69%. The chemical shift corresponding to the binding energy of Si2p was 0.91 eV, and the element fraction was 11.16%. The chemical shift corresponding to the binding energy of O1s was 1.24 eV, and the element fraction was 32.16% (which was 2.82% lower than that recorded for the ore). The chemical shift corresponding to the binding energy of C1s was 0.46 eV, and the element fraction was 29.47% (which was 12.47% higher than that recorded for the raw ore). The element fractions for Si2s and Si2p were significantly lower than the corresponding element fractions in quartz. The results indicated the chemical adsorption of Ca^{2+} and Fe^{3+} on the surface of the quartz sample and the formation of the Si-O-Ca (OH) and Si-O-Fe (OH)⁺ bonds. The formed Si-O-Ca (OH) and Si-O-Fe (OH)⁺ bonds were chemically adsorbed through the S2p orbital in SDS, and this could be attributed to the fact that the element fraction corresponding to S2p was 1.75% (Fig. 8f). The element fraction recorded for this case was higher than that recorded for the single cation-activated quartz sample. The outer layer of SDS was hydrophobic, and hence, the system could easily float. The results were arrived at by analyzing Fig. 8d and Fig. 8e. The binding energies recorded for the $\text{Ca}^{2+}/\text{Fe}^{3+}$ -activated quartz sample (binding energy for Fe2p: 711.32 eV; binding energy for Ca2p: 346.90 eV) were higher than the binding energies recorded for the single cation-activated systems. Fig. 8d presents the binding energy corresponding to Ca2p (346.93 eV), and Fig. 8e presents the binding energy corresponding to Fe2p (711.16 eV). The chemical shift corresponding to the binding energies of Si2s and Si2p recorded for the $\text{Ca}^{2+}/\text{Fe}^{3+}$ -activated quartz was high, indicating that the $\text{Ca}^{2+}/\text{Fe}^{3+}$ -activated quartz sample was more stable than the single-cation-activated quartz sample. Hence, it can be inferred that SDS forms a stable four-membered ring and a chain-like complex on the quartz surface, and this improves the extent of adsorption of the collector realized on the surface of the quartz samples.

The origin of the peak corresponding to O1s can be attributed to the quartz unit (Fig. 10(1)). A single, symmetrical peak appeared in the profile, and the maximum photoelectron intensity and peak area were recorded under these conditions. The peak corresponding to O1s in Si=O appeared at 532.68 eV. The photoelectron intensity was recorded to be 77935.01 Counts/s, and the peak area was 137958.82 CPS. eV. The symmetry of the O1s peak reduced following the interaction of the substrate with the Ca^{2+} activator (Fig. 10(2)). Results from chemical state analysis and those obtained following the Taylor peak separation method revealed that the peaks corresponding to O1s in Si=O/Ca-O and Si=O appeared at 531.97 eV. The chemical shift of the peaks was recorded, and the photoelectron intensity was reduced to 51352.65 Counts/s. The peak area decreased to 93159.35 CPS. eV. The peak corresponding to O1s in Ca-O appeared at 530.71 eV, and the photoelectron intensity was 44893.74 Counts/s. The peak area corresponding to O1s in Ca-O was 73132.91 CPS. eV. It was observed that the O atoms on the surface of the activated quartz interacted with Ca^{2+} , and chemical adsorption followed [30]. The shape of the peak corresponding to O1s changed, and the symmetry of the peak profile was lost. A substance containing the Si-O-Ca bond was formed under these conditions. After the interaction with the Fe^{3+} activator, it can be seen in Fig.10 (3). The symmetry of the O1s peak was lower. The peak corresponding to O1s in Si=O appeared at 531.95 eV, and the chemical shift was recorded to be 0.73 eV. The chemical shift corresponding to the peak presenting the O1s unit in Si=O was higher than the corresponding chemical shift recorded for the Ca^{2+} activator. The photoelectron intensity decreased to 57217.54 Counts/s, and the peak area reduced to 107121.86 CPS. eV. The peak corresponding to the O1s unit in Fe-O appeared at 529.82 eV, the photoelectron intensity was recorded to be 13877.89 Counts/s, and the peak area was found to be 29272.38 CPS. eV. It was observed that the O atoms on the activated surface interacted with Fe^{3+} , and chemical adsorption followed. This resulted in a change in the shape of the peak corresponding to O1s. The symmetry of the peak profile was lost, and the formation of the Si-O-Fe bond was observed.

Analysis of Fig. 10(4) reveals that the symmetry of the peaks corresponding to the O1s units in quartz was affected by metal ions ($\text{Ca}^{2+}/\text{Fe}^{3+}$). The symmetry decreased when the system interacted with metal ions. The chemical shift of the peak corresponding to the O1s unit in Si=O was 531.76 eV, and the photoelectron intensity decreased to 47235.05 Counts/s. The peak area decreased to 81094.54 CPD. eV. The two peaks corresponding to the O1s units in Ca-O and Fe-O appeared at 530.73 and 529.98 eV, respectively (Fig. 10(4)). The photoelectron intensities were recorded to be 11685.62 and 12828.86 Counts/s, respectively, and the peak areas were 11880.35 and 28007.67 CPS. eV, respectively. Analysis

of the results revealed that two different chemical adsorption processes proceed when metal ions ($\text{Ca}^{2+}/\text{Fe}^{3+}$) were used to activate quartz. The processes included the adsorption process proceeding through the O1s units in the Si-O-Ca and Si-O-Fe bonds, which were formed when the O atoms on quartz interacted with Ca^{2+} and Fe^{3+} .

New peaks corresponding to Ca2p and Fe2p appeared in the profiles recorded for the samples treated with activating agents (Fig. 11). (1) Peaks corresponding to $\text{Ca}2p_{3/2}$ (346.73 eV; photoelectron intensity: 23751.99 Counts/s; peak area: 39507.47 CPS. eV) and $\text{Ca}2p_{1/2}$ (350.13 eV; photoelectron intensity: 9347.86 Counts/s; peak area: 13503.11 CPS. eV) appeared. The peaks corresponding to Ca2p associated with the Ca-O and Ca-OH bonds (350.80 eV; photoelectron intensity: 3343.69 Counts/s; peak area: 5778.41 CPS. eV) were also observed in the profiles. The results indicated that the hydroxyl complex of iron was formed on the surface of the quartz sample. (2) Peaks corresponding to $\text{Fe}2p_{3/2}$ for the Ca-O bond (710.79 eV; photoelectron intensity: 7266.86 Counts/s; peak area: 26474.75 CPS. eV), $\text{Fe}2p_{1/2}$ (724.23 eV; photoelectron intensity: 3662.09 Counts/s; peak area: 13354.29 CPS. eV), and Fe2p corresponding to Fe-OH (718.00 eV; photoelectron intensity: 1740.43 Counts/s; peak area: 6346.32 CPS. eV) were observed in the profiles. The results revealed that the hydroxyl complex of iron was formed on the surface of the quartz sample.

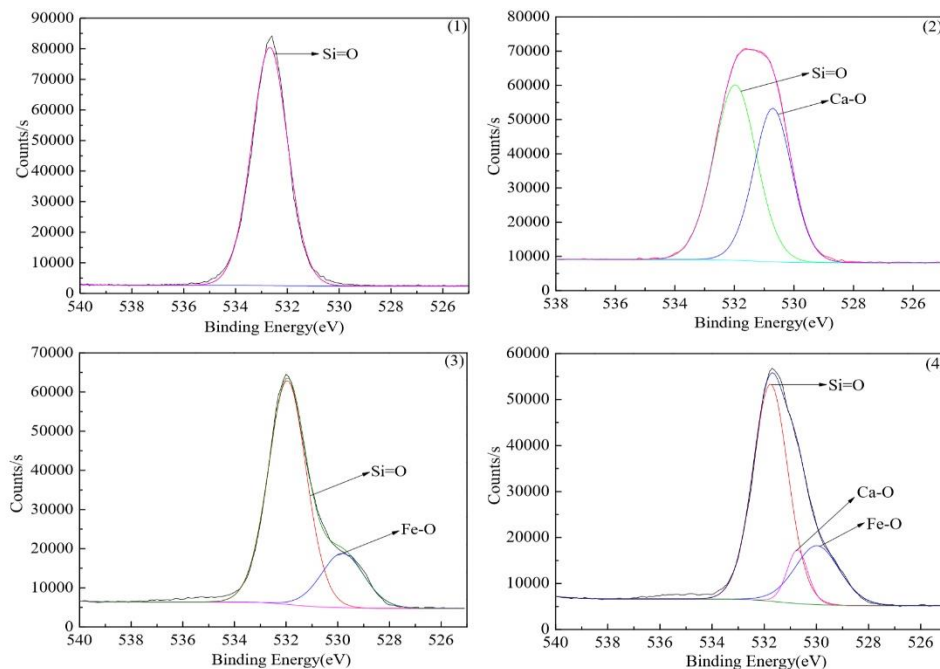


Fig. 10. High-resolution spectral profiles recorded for the O1s units using the XPS technique. The profiles were recorded before and after quartz interacted with SDS

The data were processed following data processing and Taylor peak separation methods. (3) Peaks corresponding to $\text{Ca}2p_{3/2}$ (346.45 eV; photoelectron intensity: 6532.82 Counts/s; peak area: 10743.10 CPS. eV), $\text{Ca}2p_{1/2}$ (349.84 eV; photoelectron intensity: 1921.65 Counts/s; peak area: 2539.23 CPS. eV), and Ca2p (350.19 eV; photoelectron intensity: 1319.49 Counts/s; peak area: 2644.85 CPS. eV) were observed in the profiles. The results revealed that the hydroxyl complex of calcium was formed on the surface of the quartz sample. (3) Peaks corresponding to $\text{Fe}2p_{3/2}$ (710.56 eV; photoelectron intensity: 4439.81.86 Counts/s; peak area: 19106.29 CPS. eV), $\text{Fe}2p_{1/2}$ (724.41 eV; photoelectron intensity: 2215.96 Counts/s; peak area: 10713.78 CPS. eV), and Fe2p for the Ca-O and Fe-OH bonds (716.83 eV; photoelectron intensity: 810.21 Counts/s; peak area: 4026.98 CPS. eV) were observed in the profiles. This indicated that the hydroxyl complex of iron was formed on the surface of quartz [27]. Analysis of the data revealed that the O atoms on the surface of the quartz sample interacted with $\text{Ca}^{2+}/\text{Fe}^{3+}$, resulting in the simultaneous formation of the Si-O-Ca and Si-O-Fe bonds. The number of active sites on the quartz surface increased, the diversity increased, and SDS could be readily adsorbed on the quartz surface under these conditions.

162262

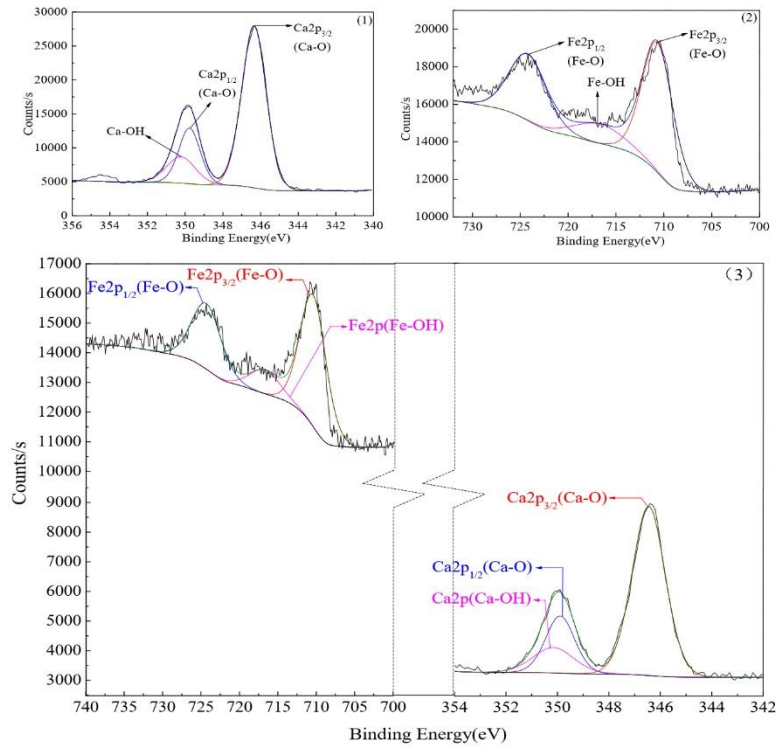


Fig. 11. Profiles recorded for Ca2p and Fe2p following the interaction between quartz and activator

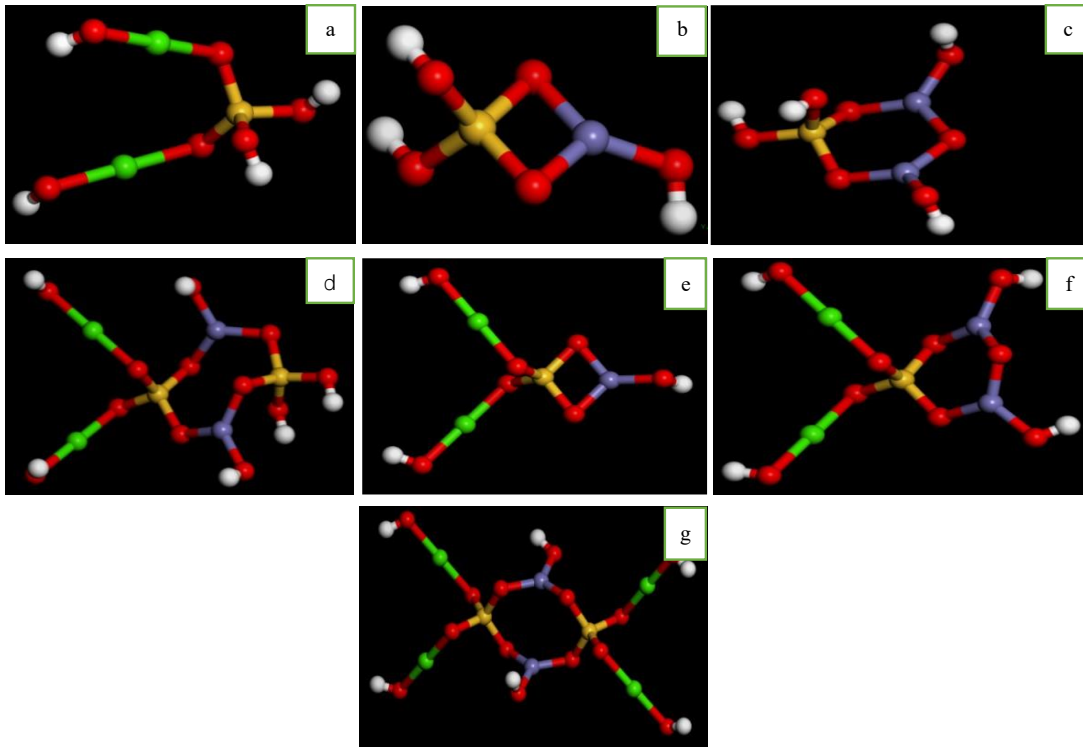


Fig. 12. Possible configurations adopted during the interaction between the activator and quartz (a. Quartz and Ca^{2+} form a chain structure; b. Quartz and Fe^{3+} constitute a four-membered ring; c. Quartz and Fe^{3+} form a six-membered ring; d. Quartz and $\text{Ca}^{2+}/\text{Fe}^{3+}$ form an eight-membered ring with two chain ligands; e. Quartz and $\text{Ca}^{2+}/\text{Fe}^{3+}$ form a four-membered ring with two chain ligands; f. Quartz and $\text{Ca}^{2+}/\text{Fe}^{3+}$ form a six-membered ring with two chain ligands; g. Quartz and $\text{Ca}^{2+}/\text{Fe}^{3+}$ form an eight-membered ring with four chained ligands) (Yellow presents Si; Blue presents Fe^{3+} ; Green presents Ca^{2+} ; Oxygen atoms are presented in red; White presents hydrogen atoms)

New peaks corresponding to Ca2p and Fe2p appeared in the XPS profiles when the Ca²⁺/Fe³⁺ system was used as the ion activator. Results obtained from solution chemistry and zeta potential analysis and those obtained using the FT-IR and XPS techniques revealed that the hydroxyl group on the surface of the quartz unit was deprotonated, and these coordinated with the monovalent hydroxyl calcium systems to form a Si-O-CaOH bond when Ca²⁺ was used to activate quartz at a pH of 12. Si-O-CaOH functions as the activation site and the physical adsorption process is initiated under these conditions. The probable configuration of the activator realized during the process of adsorption is shown in Fig. 12a. Fig. 12a reveals the formation of an unstable chain structure. When Fe³⁺ activates quartz at a pH of 7, the Fe(OH)₃ precipitate is formed as the dominant component. The two hydroxyl groups present on the quartz surface are deprotonated, and the hydroxyl groups on the precipitate undergo dehydration to form the Si-O-Fe bonds, which are physically adsorbed in the presence of anion collectors. Quaternary and quinary chelates are formed when coordination occurs via the O atoms on the surface of the quartz sample. The possible configurations are shown in Fig. 12b and Fig. 12c. When the Ca²⁺/Fe³⁺ system synergistically activates quartz, the peaks corresponding to the O1s units in the two metal-oxygen species appear in the profiles simultaneously, indicating that both the metal ions act as activators. The probable configurations are shown in Fig. 12d, e, f, and g. The cyclic chelate complexes vary in their stability.

It has been previously reported [31-32] that the instability of the tetracyclic ring can be attributed to the excess tension in the compounds. Bayer proposed a two-point theory: [31-32] (1) all cyclic compounds present a planar structure, and (2) the bond angle in these compounds differs from the normal bond angle of an sp³ hybrid orbital (109° 28'). The multi-membered ring formed was stable, and the stability could be attributed to the first hypothesis of Bayer's theory. Nuclear magnetic resonance spectroscopy and other techniques have been used to characterize various samples over the years. It is now known that a multi-membered compound may not present a planar structure. This explains the stability of the multi-membered chelates. The probable configurations adopted during the interaction between the activator and quartz during adsorption have been presented in Fig. 12. Analysis of Fig. 12 revealed that the chain structure was the most unstable of the lot. Analysis of the double electron layer reveals that quartz interacts with Ca²⁺ in the slip layer, resulting in the instability of the complex. The tension associated with the four-membered ring is significantly high (Fig. 12b), resulting in the instability of the rings. The chelate complexes (Fig 12c and d) are more stable than the others. Quartz and Fe³⁺ interacted in the tight layer. This explains the stability of the complex presented in Fig. 11c. If the ring contains less than 4 members and more than 7 members, the possibility of forming a closed ring in conjugated complexes decreases [31-32]. A stable chelate consisting of a six-membered ring and a chain ligand is formed through the formation of the metal-oxygen-silicon bonds (Fig. 12e, f, and g).

The most probable configurations adopted when the Ca²⁺, Fe³⁺, and composite activators are used have been presented in Fig. 12a, c, and f, respectively.

4. Conclusions

The results from micro-flotation tests revealed that the surface of quartz could be activated by different degrees in the presence of different metal-based activators. Different dominant components were formed from different metal ion activators when SDS was used to float quartz. The combined Ca²⁺/Fe³⁺ system performed better than single metal ions in terms of surface activation. The flotation recovery recorded was close to 100% when the combined system was used. Results from solution chemical calculations and zeta potential analysis revealed that the Ca(OH)⁺ units were formed as the dominant component when Ca²⁺ was used as the activator of the quartz surface in the pH range of 8-12. The results agreed well with the results obtained by analyzing the data recorded during quartz flotation. The flotation recovery of quartz was recorded to be 75.5% when the dominant component was Ca(OH)⁺. Fe(OH)_{3(s)} was formed as the dominant component when Fe³⁺ activated the surface of quartz in the pH range of 7-9. The results agreed well with the results obtained by analyzing the data obtained during the flotation of quartz. The flotation recovery was recorded to be 96.3% under these conditions. It was observed that SDS significantly affected the flotation behavior of quartz when the Ca²⁺/Fe³⁺ system was used to activate the surface of quartz at a pH of 8. The flotation recovery recorded under these conditions was 98.5%. The results revealed that Ca(OH)⁺ and Fe(OH)_{3(s)} were produced as the dominant

components on the surface of quartz when the $\text{Ca}^{2+}/\text{Fe}^{3+}$ system was used for surface activation. When the pH was in the range of 6–9, The flotation recovery was >90%. Thus, the synergistic effect of the components produced following the hydrolysis of $\text{Ca}^{2+}/\text{Fe}^{3+}$ helped activate the surface of the quartz sample. The pH range could be expanded, and the quartz recovery rate could be improved. The sample activated using the $\text{Ca}^{2+}/\text{Fe}^{3+}$ system exhibited higher adsorption ability than the single-cation-activated quartz sample. The pH value could be readily controlled as the pH range was widened.

Results obtained using the FT-IR and XPS techniques revealed that the use of Ca^{2+} , Fe^{3+} , and combined $\text{Ca}^{2+}/\text{Fe}^{3+}$ could improve the degree of adsorption of quartz by SDS. The synergistic activation realized in the presence of the combined activator was stronger than the effect exerted by a single metal ion. The active sites Si-O-Ca(OH) and Si-O-Fe(OH)⁺ acted simultaneously to exert the observed effects. The adsorption of SDS on the surface of the quartz sample, under the action of the combined $\text{Ca}^{2+}/\text{Fe}^{3+}$ system, proceeded via physical as well as chemical adsorption processes. MS software was used to determine the possible configurations adopted by the activator during its adsorption on the quartz surface. It was concluded that a chain-like configuration was adopted in the presence of the Ca^{2+} activator, a six-membered chelate complex was formed in the presence of the Fe^{3+} activator, and a six-membered chelate ring with a chain–ligand configuration was formed in the presence of the $\text{Ca}^{2+}/\text{Fe}^{3+}$ activator.

Acknowledgments

The study was funded by the Inner Mongolia Autonomous Region Science and Technology Plan Project (Grant No.2021GG0438), Inner Mongolia Natural Science Foundation (2020MS05048, 2020BS05029), and Fund Project National Key R & D Program (Rare Earth Based Solid Waste Resource Properties, Precision Mining and Ecological Environmental Impact Assessment) (2020YFC1909101).

References

- WANG, Y., 2014. China Mining Science and Technology Wenhui. Beijing: Metallurgical Industry Press
- GONG, G., HAN, Y., GAO, P., 2017. *Research progresses of preparation technology of super iron concentrate*. Conservation and Utilization of Mineral Resources, (1) : 103-107
- ZHANG, H., LIU W., HAN C., 2018. *Effects of monohydric alcohols on the flotation of magnesite and dolomite by sodium oleate*. Journal of Molecular Liquids, 249.
- YAO, J., SUN, H., YANG, B, 2020. *Selective co-adsorption of a novel mixed collector onto magnesite surface to improve the flotation separation of magnesite from dolomite*. Powder Technology, 371.
- ZHANG, H., LIU, W., HAN, C., 2018. *Intensify dodecylamine adsorption on magnesite and dolomite surfaces by monohydric alcohols*. Applied Surface Science, 444.
- LIU, W., PENG, X., LIU, W., 2020. *Effect mechanism of the iso-propanol substituent on amine collectors in the flotation of quartz and magnesite*. Powder Technology, 360.
- SHI, Y., QIU, G., HU, Y., 2001. *Surface chemical reactions in oleate flotation quartz*. Mining and Metallurgical Engineering, (3):43-45.
- WANG, D., HU, Y., 1990. *The Investigation of role of surface precipitation of meta hydroxide in flotation of quartz*. Journal of Central South University of Mining and Metallurgy, (3): 248-253.
- FUERSTENAU, M.C., GAUDIN, A.M. 1976. *Flotation: A.M. Gaudin memorial volume*. Toronto: Toronto Public Library,
- FUERSTENAU, M.C., 1963. *The role of metal ion hydrolysis in sulfonate flotation of quartz*. Transaction of American Institute of Mining, Metallurgical, and Petroleum Engineers, 226:449.
- EJTEMAEI, M., IRANNAJAD, M., GHARABAGHI, M., 2012. *Role of dissolved mineral species in selective flotation of smithsonite from quartz using oleate as collector*. International Journal of Mineral Processing, (8):40-47.
- SUN, C., 2001. *Flotation Principle of Silicate Minerals*. Beijing: Science Press.
- WANG, J., YIN, W., LI, Z., 2017. *Influence and mechanism of lead and ferric ions on the flotation of scheelite and quartz*. Conservation and Utilization of Mineral Resources, (2):35-38.
- TANG, S., ZHANG, L., ZHANG, C., 2017. *Study on activation of sodium dodecyl sulfonate collection quartz by Fe^{3+}* . Non-Metallic Mines, (5), 79-81.
- YIN, R.M, CHEN, L.Z, HOU, Q.L, 2013. *Research on flotation mechanism of quartz using magnesium ion as activator*. Journal of Functional Materials, (15):621-625.
- MENG, Q.Y., FENG, Q.M., OU, L. M, 2016. *Flotation behavior and adsorption mechanism of fine wolframite with octyl*

- hydroxamic acid*. Journal of central south university, 23(6):1339-1344.
- CHILUKOTI, H.K., KIKUGAWA, G., OHARA, T., 2014. *Structure and transport properties of liquid alkanes in the vicinity of α -quartz surfaces*. International journal of heat and mass transfer, 79(12):846-857.
- LAMBERSON, L., RAMESH, K.T., 2015. *Spatial and temporal evolution of dynamic damage in single crystal-quartz*. Mechanics of materials, 87(8):61-79.
- LIU, A., FAN, J.C., FAN, M.Q., 2015. *Quantum chemical calculations and molecular dynamics simulations of amine collector adsorption on quartz (001) surface in the aqueous solution*. International journal of mineral processing, 134(1):1-10.
- SAHOO, H., SINHA, N., RATH, S., 2015. *Ionic liquids as novel quartz collectors: Insights from experiments and theory*. Chemical engineering journal, 273(1), 46-54.
- WANG, L., SUN, W., HU, Y.H., 2014. *Adsorption mechanism of mixed cationic/anionic collector in muscovite-quartz flotation system*. Minerals engineering, 64, (1), 44-55.
- TJAMES, R.O., HEALY, T. W., 1972. *Adsorption of hydrolyzable metal ions at the oxide-water interface. I. Co(II) adsorption on SiO_2 and TiO_2 as model systems*. Journal of Colloid & Interface Science, 40, 42-52.
- ZACHARA, J.M., COWAN, C.E., RESCH, C.T., 1991. *Sorption of divalent metals on calcite*. Geochimica et Cosmochimica Acta, 55(6), 1549-1562.
- ZHOU, Y., HU, Y., WANG, Y., 2011. *Effect of metallic ions on dispersibility of fine diasporite*. Transactions of Nonferrous Metals Society of China, 21(5), 1166-1171.
- WENG, S.P., 2016. *Fourier transform infrared spectroscopy*. Beijing: Chemical Industry Press; 426-428.
- GUO, Y., KOU, J., SUN, T., XU, C., 2015. *Xu Shihong. Adsorption mechanism of sodium dodecyl sulfate and lauric acid on quartz by QCM-D*. Mining and Metallurgical Engineering, 35(2), 50-54.
- SUN, Z., FORSLING, W., CHEN, J., 1992. *Complexation of metal ions at the quartz/water interface and its influence on quartz flotation*. The Chinese Journal of Nonferrous Metals, 2(2), 15-20.
- SMITH, 2007. *Advanced organic chemistry*. London: Advanced organic chemistry, part A.
- ZHANG, J., WANG, W., LIU, J., HUANG, Y., FENG, Q., ZHAO, H., 2014. *Fe(III) as an activator for the flotation of spodumene, albite, and quartz minerals*. Minerals Engineering, 61:16-22.
- EJTEMAEI, M., IRANNAJAD, M., GHARABAGHI, M., 2012. *Role of dissolved mineral species in selective flotation of smithsonite from quartz using oleate as collector*. International Journal of Mineral Processing, 114:40-47.
- ZHANG, J., WANG, X., 2008. *Mine Pharmacy*. Beijing: Metallurgical Industry Press, 428, 452.